JPET Fast Forward. Published on March 24, 2004 as DOI: 10.1124/jpet.104.066654
This article has not been copyedited and formatted. The final version may differ from this version.

Role of Adenosine A_1 Receptor in the Regulation of Gastrin Release

Linda Yip, Henry Chi Hang Leung and Yin Nam Kwok

Department of Physiology, University of British Columbia, 2146 Health Sciences Mall, Vancouver, BC, Canada. V6T 1Z3

Running Title: Adenosine A_1 receptors and Gastrin Release

Corresponding Author: Yin Nam Kwok Ph.D., Department of Physiology, University of British Columbia, 2146 Health Sciences Mall, Vancouver, BC. Canada. V6T 1Z3. Tel: 604-822-6228, Fax: 604-822-6048, email: kynkwok@interchange.ubc.ca

Number of pages text: 37

Number of tables: 0

Number of figures: 8

Number of references: 38

Number of words (Abstract 248; Introduction 705; Discussion 1433)

Non-standard abbreviations used in paper: N^6-cyclopentyladenosine (CPA), 2-p-(2-carboxyethyl)phenethylamino-5'N-ethylcarboxamidoadenosine (CGS 21680), 1-deoxy-1-[6-[[(3-iodophenyl)methyl]amino]-9H-purin-9-yl]-N-methyl-ß-D-ribofuranuronamide (IB-MECA), 8-cyclopentyl-1,3-dipropylxanthine (DPCPX), 3,7-dimethyl-1-propargylxanthine (DMPX), immunoreactive gastrin (IRG), somatostatin-like immunoreactivity (SLI), reverse transcription-polymerase chain reaction (RT-PCR), bovine serum albumin (BSA), radioimmunoassay (RIA), 6-carboxyfluorescein (FAM), 6-carboxytetramethylrhodamine (TAMRA), uracil-N-glycosylase (UNG), threshold cycle (C_T), protein gene product 9.5 (PGP 9.5), von Willebrand's factor (VWF), A_1 receptor-immunoreactivity (A_1R-IR), immunoreactivity (IR), phosphate buffered saline (PBS), Tris buffered saline (TBS), polyvinylidene fluoride (PVDF), and Tris acetate EDTA (TAE).

Recommended section assignment: Gastrointestinal, hepatic, pulmonary & renal

JPET Fast Forward. Published on March 24, 2004 as DOI: 10.1124/jpet.104.066654
This article has not been copyedited and formatted. The final version may differ from this version.

Abstract

Adenosine has been demonstrated to inhibit gastric acid secretion. In the rat stomach, this inhibitory effect may be mediated indirectly by the inhibition of gastrin release. Results show that the A_1 receptor agonist, N^6-cyclopentyladenosine (CPA), suppressed immunoreactive gastrin (IRG) release in a concentration-dependent manner. CPA significantly inhibited IRG release at 0.001 μM, and maximally inhibited IRG release at 1 μM. At concentrations of 0.001 to 0.1 μM, the A_{2A} receptor-selective agonist, 2-p-(2-carboxyethyl)phenethylamino-5'-N-ethylcarboxamidoadenosine and A_3 receptor-selective agonist, 1-deoxy-1-[6-[[(3-iodophenyl)methyl]amino]-9H-purin-9-yl]-N-methyl-ß-D-ribofuranuronamide, had no effect on IRG release, suggesting the involvement of A_1 receptors. In agreement, the A_1 receptor-selective antagonist, 8-cyclopentyl-1,3-dipropylxanthine, abolished adenosine-induced inhibition of IRG release. Results of immunohistochemistry experiments reveal the presence of A_1 receptor immunoreactivity on mucosal G-cells and D-cells, and the gastric plexi, but not parietal cells, suggesting that adenosine may act directly on G-cells or indirectly on the gastric plexi to modulate IRG release. The structure of the mucosal A_1 receptor was found to be identical to that in the rat brain. Alternative splicing within the coding region of this receptor did not occur. A real-time reverse transcription-polymerase chain reaction assay was developed to measure gastric A_1 receptor gene expression. The highest level of gastric A_1 receptor mRNA was found in the corporeal muscle. However, this level was significantly lower in comparison to the striatum. In conclusion, this study shows that adenosine may suppress IRG release, at least in part, by activating A_1 receptors localized on G-cells, and may consequently result in an inhibition of gastric acid secretion.

In the stomach, adenosine has been demonstrated to protect against stress-induced gastric ulcer formation (Geiger and Glavin, 1985; Westerberg and Geiger, 1987). This protective effect may be attributed to the inhibitory action of adenosine on gastric acid secretion. The administration of adenosine and its analogs was shown to inhibit gastric acid secretion in various species (Gerber et al., 1985; Heldsinger et al., 1986; Glavin et al., 1987; Gerber and Payne, 1988; Westerberg and Geiger, 1989). However, the site at which adenosine acts to suppress acid secretion appears to differ. In guinea pigs (Heldsinger et al., 1986) and dogs (Gerber et al., 1985; Gerber and Payne, 1988), adenosine was shown to act directly on the acid-secreting parietal cells to inhibit acid secretion. In dogs, adenosine also suppressed the release of gastrin, a potent gastric acid secretagogue (Schepp et al., 1990). In rats, adenosine was shown not to alter basal or histamine-stimulated aminopyrine uptake in isolated enriched parietal cell preparations (Puurunen et al., 1987). Thus, adenosine is unlikely to act directly on the parietal cells to inhibit acid secretion in the rat stomach. Instead, our laboratory has demonstrated that adenosine may suppress gastric acid secretion indirectly by modulating the release of gastrin and somatostatin (Kwok et al., 1990). Adenosine was found to inhibit immunoreactive gastrin (IRG) release from the isolated vascularly perfused rat stomach in a concentration-dependent manner (Kwok et al., 1990). This nucleoside was also able to inhibit basal and abolish carbachol-stimulated gastrin release from rat antral mucosal fragments (Harty and Franklin, 1984), and to suppress carbachol- and norepinephrine-stimulated gastrin release from rat antral mucosal cells (DeSchryver-Kecskemeti et al., 1981). In addition, adenosine deaminase, a metabolic enzyme of adenosine, was shown to enhance basal and carbachol-stimulated gastrin release (Harty and Franklin, 1984), while theophylline, a non-selective adenosine antagonist, blocked the inhibitory effect of adenosine on carbachol- and norepinephrine-stimulated gastrin release (DeSchryver-Kecskemeti

et al., 1981). These studies suggest that the action of adenosine is unlikely due to its vascular effect and endogenous adenosine may act on extracellular adenosine receptors to inhibit gastrin release, leading to a subsequent inhibition of gastric acid secretion.

Adenosine elicits its effects by acting on G-protein-coupled receptors belonging to the purinergic P1 receptor family. These receptors are classified into adenosine A_1, A_{2A}, A_{2B}, and A_3 subtypes based on their pharmacological and structural properties (Fredholm et al., 2001). In rats, the adenosine receptor subtype(s) involved in modulating IRG release has not been characterized. Thus, the first objective of the present study was to determine the adenosine receptor subtype involved in the inhibitory action of adenosine on IRG release in the isolated vascularly perfused rat stomach using selective adenosine agonists and antagonists.

A low level of A_1 receptor gene expression has previously been found in the whole rat stomach using reverse-transcription polymerase chain reaction (RT-PCR) (Dixon et al., 1996). However, the expression of this receptor in functionally distinct regions of the stomach is undetermined. Although our preliminary results suggest that adenosine A_1 receptors may be involved in the inhibition of IRG release, the cellular localization of these receptors on specific cells of the stomach, such as the gastrin-secreting G-cells has also not been examined. Therefore, the second objective of this study was to determine the cellular localization, distribution and gene expression level of the A_1 receptor in the rat stomach using immunohistochemistry, RT-PCR, and real-time RT-PCR, respectively. The adenosine A_1 receptor has been cloned in tissues of various species including the human and rat brain (Ralevic and Burnstock, 1998), but structural information regarding the rat gastric A_1 receptor is lacking. Northern blot analysis has demonstrated the presence of two A_1 receptor mRNA transcripts in the rat stomach (Mahan et al., 1991; Reppert et al., 1991). However, it is unclear if these transcripts differ in their coding

regions. Differences in the coding region may result in the production of multiple forms of the receptor. Previous studies have shown that multiple variants of the rat A_3 receptor were generated by alternative splicing in the coding region of the A_3 receptor gene (Sajjadi et al., 1996). Since multiple forms of the A_1 receptor may have important functional implications, the final objective of this study was to clone and sequence the entire coding region of the mucosal A_1 receptor gene.

JPET Fast Forward. Published on March 24, 2004 as DOI: 10.1124/jpet.104.066654
This article has not been copyedited and formatted. The final version may differ from this version.

Materials and Methods

Stomach perfusion

Animals were treated in accordance with the guidelines of the University of British Columbia Committee on Animal Care. Male Wistar rats (250 to 325 g) were housed in light- and temperature-controlled rooms with free access to food and water. Prior to stomach perfusion, animals were deprived of food but not water for at least 14 h. Rats were anesthetized with an i.p. injection (60 mg/kg) of sodium pentobarbital (Somnotol®, MTC Pharmaceuticals, Cambridge, ON, Canada). The surgical procedures used to isolate the stomach for perfusion have previously been described (Pederson et al., 1984; Kwok et al., 1990). The stomach was exposed by an abdominal midline incision. The superior mesenteric artery and vasculatures supplying the left and right adrenal glands and kidneys were occluded or cut between double ligatures. The spleen and pancreas were then dissected along the greater curvature of the stomach. Care was taken to preserve the right gastroepiploic artery. A cannula was secured into the gastroduodenal junction to allow for drainage of gastric contents. The pancreas, spleen, small and large intestines were then removed. Arterial perfusion was achieved by inserting a cannula into the aorta with the tip lying adjacent to the celiac artery. Perfusate was introduced into the stomach via this arterial cannula, followed by an injection of 2 ml saline containing 600 U of heparin (Sigma, St. Louis, MO). Venous effluent was collected via a portal vein cannula. Stomach preparations were equilibrated for 30 min before 5-min samples were collected into ice-cold scintillation vials containing 0.3 ml of Trasylol® (aprotinin, 10,000 KIU/ml; Miles Labs., Etobicoke, ON). Aliquots (1 ml) were immediately transferred into ice-cold test tubes and stored at -20°C until assayed.

The stomach was perfused at a rate of 3 ml/min using a peristaltic pump (Cole-Parmer Instrument Co. Chicago, IL). The perfusate was composed of Krebs' solution (in mM: NaCl, 120; KCl, 4.4; $CaCl_2$, 2.5; $MgSO_4 \cdot 7H_2O$, 1.2; KH_2PO_4, 1.5; $NaHCO_3$, 25 and dextrose, 5.1) containing 0.2% BSA (RIA grade; Sigma) and 3% dextran (Clinical grade; Sigma). The perfusate was continuously gassed with a mixture of 95% O_2 and 5% CO_2 to maintain a pH of 7.4. Both the perfusate and the preparation were kept at 37^{o}C by thermostatically-controlled heating units throughout the experiment. Drugs were introduced into the perfusate via side-arm infusion at a rate calculated to give the final perfusion concentrations. The following drugs were purchased from Sigma-Aldrich: adenosine hemisulphate salt, N^6-cyclopentyladenosine (CPA), 2-p-(2-carboxyethyl)phenethylamino-5'N-ethylcarboxamidoadenosine HCl (CGS 21680), 1-deoxy-1-[6-[[(3-iodophenyl)methyl]amino]-9H-purin-9-yl]-N-methyl-ß-D-ribofuranuronamide (IB-MECA), 8-cyclopentyl-1,3-dipropylxanthine (DPCPX) and 3,7-dimethyl-1-propargylxanthine (DMPX). Adenosine analogs were first dissolved in a small volume of dimethyl sulfoxide (BDH, Toronto, ON) and subsequently diluted with saline or perfusate to 0.03 or 0.5% before perfusing into the stomach. At these concentrations, dimethyl sulfoxide did not alter basal IRG release.

Radioimmunoassay (RIA) and data analysis

The specific RIA employed for the measurement of IRG has previously been described (Jaffe and Walsh, 1978; Fujimiya and Kwok, 1997). The gastrin antibody (PM1) was kindly provided by Dr. R. Pederson (Physiology, UBC). The drugs used in the present study did not cross-react with this antibody. The inter- and intra-assay variations were shown to be less than 6 and 4%, respectively.

JPET Fast Forward. Published on March 24, 2004 as DOI: 10.1124/jpet.104.066654
This article has not been copyedited and formatted. The final version may differ from this version.

Although the basal rate of IRG release varied among animals, previous experiments have demonstrated that basal IRG release was maintained in the perfused rat stomach (Pederson et al., 1984; Kwok et al., 1990). Therefore, results were expressed as mean ± SEM of IRG release (%), which was calculated as follows: [IRG release (pg/min) during a 5 min period ÷ IRG release (pg/min) during period 1] × 100. To compare the effect of analogs, results were also expressed as percentage (%) inhibition (IRG release), which was calculated as follows: [mean basal IRG release (periods 1-3) – mean IRG release in the presence of drug (periods 4-7)] pg/min ÷ [mean basal IRG release (periods 1-3)] pg/min × 100. Percent (%) change was calculated as follows: [mean IRG release in the presence of drug (periods 4-7) – mean basal IRG release (periods 1-3)] pg/min ÷ [mean basal IRG release (periods 1-3)] pg/min × 100. Statistical significance ($P < 0.05$) was determined using one-way analysis of variance followed by Dunnett's multiple comparison test, and the paired or unpaired Student's t-test when appropriate. Statistics and estimation of the EC_{50} were performed using GraphPad Prism (v. 3.0, GraphPad software, San Diego, CA).

Immunohistochemistry

Gastric corporeal and antral tissues from male Wistar rats were fixed overnight, cryoprotected, and sectioned as previously described (Yip et al., 2003). Free-floating sections (30 μm) were sequentially incubated in 0.1 M PBS containing 50 mM NH_4Cl (30 min), 0.1 M PBS containing 100 mM glycine (10 min), and blocking buffer (0.1 M PBS containing 1% BSA and 0.3% Triton X-100, 1 h). Antibodies were diluted in blocking buffer containing 0.1% sodium azide. Tissue sections were incubated with the rabbit anti-A_1 adenosine receptor antibody (1:500; Sigma-Aldrich) for 72 h at 4ºC, washed with 0.1 M PBS (3 × 15 min), and then incubated with donkey anti-rabbit IgG conjugated to cyanine Cy3 (1:2,000; Jackson ImmunoReasearch, West Grove,

PA) overnight at 4°C. Sections were again washed and either double stained or mounted onto glass slides. For double staining, tissue sections were incubated with another primary antibody for 72 h at 4°C, washed, and incubated with Alexa Fluor 488-conjugated secondary antibody overnight at 4°C. Sections were then washed, mounted onto glass slides, coverslipped using a mixture of 0.1 M PBS in glycerin (1:9), and sealed with nail polish.

Control experiments for immunohistochemistry

The A_1 receptor antibody has been shown to cross-react with rat A_1 receptors and its specificity has previously been examined in rat tissues (Carruthers et al., 2001). Western blotting and immunoneutralization experiments were also performed in the present study to examine the specificity of this antibody on rat gastric tissues. Additional negative control experiments were also performed to confirm that A_1 receptor-immunoreactivity (A_1R-IR) does not result from non-specific binding of the secondary antibodies.

Western Blotting: Protein was extracted from the rat fundus, corpus, antrum and the brain using Trizol® Reagent, according to manufacturer's instructions. Protein samples were re-dissolved in 1% sodium dodecyl sulphate at 50°C, and concentrations were determined using the BCA assay kit (Pierce Biotechnology, Rockford, IL). Protein samples (10 μg) were denatured in 1× sodium dodecyl sulphate gel loading buffer [50 mM Tris-Cl (pH 6.8), 100 mM dithiothreitol, 2% sodium dodecyl sulphate, 0.1% bromphenol blue and 10% glycerol] by boiling for 5 min. Samples were loaded and resolved on polyacrylamide gels composed of a 4% stacking and 10% separating gel, and then transferred to polyvinylidene fluoride (PVDF) membranes (Bio-Rad, Richmond, CA). The methods used for electrophoresis and immunoblotting have previously been described (Sambrook et al., 1989). PVDF membranes were washed in Tris-buffered saline

(TBS) and incubated in blocking buffer (TBS containing 0.1% Tween 20, and 5% BSA) for 1 h at room temperature with shaking. Membranes were then washed and incubated with the anti-A_1 adenosine receptor antibody overnight at 4°C. This primary antibody was diluted to 1:5,000 with TBS containing 0.1% Tween 20 (TBST) prior to use. Membranes were washed in TBS and then incubated in TBST containing anti-rabbit horseradish peroxidase-conjugated secondary antibody (1:20,000; Jackson ImmunoResearch, West Grove, PA) for 1 h at room temperature with shaking. Membranes were then washed in TBST and enhanced chemiluminescence immunodetection was performed according to manufacturer's instructions (Amersham Pharmacia Biotech, England). Results show that two immunoreactive products with apparent molecular mass of 40.5 and 67 kDa were detected (Fig. 1). These findings are consistent with the results of Western blot experiments performed in rat trigeminal ganglion neurons using the same antibody (Carruthers et al., 2001). The larger immunoreactive product likely represents the glycosylated form of the A_1 receptor since deglycosylation can shift the molecular mass of the larger product to ~40 kDa, the expected size of the A_1 receptor (Carruthers et al., 2001).

Immunoneutralization of the A_1 receptor antibody: Immunoneutralization experiments were also performed in the present study to confirm the specificity of the antibody. Since the blocking peptide for the A_1 receptor antibody is unavailable from the supplier, one was synthesized by the Nucleic Acid Protein Services Unit at UBC. The amino acid sequence (Cys-Gln-Pro-Lys-Pro-Pro-Ile-Asp-Glu-Asp-Leu-Pro-Glu-Glu-Lys-Ala-Glu-Asp) of this synthetic peptide was based on the immunogen sequence provided by Sigma-Aldrich. The lack of homology between the sequence of the blocking peptide and other proteins was confirmed using the BLAST software featured at the NIH National Center for Biotechnology Information website. The only proteins

which expressed high homology (>70%) with this peptide are A_1 receptors from various species. The rat A_{2A}, A_{2B} and A_3 receptor sequences exhibit no significant similarity. The blocking peptide was dissolved in 0.1 M PBS (pH 7.4) and the concentration was determined using the BCA assay. The A_1 receptor antibody was neutralized by incubating 1 µl of the stock antibody with 0.1 µg of the blocking peptide in 0.5 ml 0.1 M PBS containing 1% BSA, 0.3% Triton X-100, and 0.1% sodium azide for 48 h at 4°C. A positive control lacking the blocking peptide was also prepared. Tissues stained with the neutralized antibody did not demonstrate A_1R-IR, while tissues stained with the positive control demonstrated extensive A_1R-IR (see Fig. 5).

Controls for non-specific binding: Additional control experiments were also performed to ensure that non-specific binding did not occur. Experiments included incubating sections with 1% BSA in place of the primary antibody, incubation without the secondary antibody, or incubation with Alexa 488-conjugated anti-mouse IgG secondary antibody or Cy3-conjugated anti-rabbit IgG secondary antibody alone. No immunoreactivity (IR) was observed following these procedures (Fig. 5).

Double staining

For double staining experiments, monoclonal primary antibodies against somatostatin (1:500; Soma 8, MRC Regulatory peptide group, UBC), gastrin (1:30,000; 109-21 provided by the late Dr. John Walsh), protein gene product 9.5 (PGP 9.5; 1:200; ab8189, Abcam Limited, Cambridge, UK), human von Willebrand's factor (VWF; 1:50; Serotec, Oxford, UK) and H^+K^+-ATPase β (1:2,000; Affinity Bioreagents Inc., Golden, CO) were used.

Confocal Microscopy

Stained tissue sections were viewed using the Biorad Radiance 2000 confocal scanning laser system mounted on a Nikon Eclipse TE300 inverted microscope. A krypton gas laser with an excitation wavelength of 568 nm and emission filter of 575-625 nm (for visualization of Cy3), and an excitation wavelength of 488 and emission filter of 500-530 nm (for visualization of Alexa Fluor 488) was used. Bleed-through was not detected for any of the antibodies. Lens magnification of ×40 was used with a zoom factor of 1.0 and z-step of 0.5 to 1.0 μm, while lens magnification of ×60 was used with a zoom factor of 1.0 to 1.6 and a z-step of 0.3 to 0.5 μm. The software program Lasersharp 2000 (v. 4.1, Biorad, Hercules, CA) was used to scan tissue sections sequentially using the red and green collection channels and the Kalman collection filter (n=2). Images with a resolution of at least 512 × 512 pixels were obtained and then analyzed using NIH image (National Institutes of Health, Bethesda, MD, USA) and Adobe Photoshop (v. 7.0, Adobe systems, San Jose, CA). To determine whether co-localization occurred, the image collected from the red channel (A_1R-IR) was overlaid on the image collected from the green channel (somatostatin, gastrin, VWF, PGP 9.5, or H^+K^+-ATPase β-IR) using Adobe Photoshop. Co-localization of A_1R-IR with gastrin-IR and somatostatin-IR was quantified in the antral and/or corporeal mucosa by examining at least 3 tissue sections from 4 different animals.

RT-PCR

Primer design and synthesis

PCR primers were designed based on previously published rat brain A_1 receptor cDNA sequences (Accession number: M64299) (Mahan et al., 1991) using the software program PCGene (IntelliGenetics, Mountainview, CA). The forward and reverse primer sequences were

5' GTC TGC TGA TGT GCC CAG CT3' (corresponding to position 322-341 bp of the rat brain A_1 receptor cDNA sequence) and 5' ACA GGG TGG GAC AGG GAG AA 3' (corresponding to position 1388-1407 bp), respectively. The amplicon generated (1086 bp) spans the entire coding region of the A_1 receptor gene. The primers were synthesized by the Nucleic Acid Protein Services Unit at UBC.

Tissue and total RNA extraction

Male Wistar rats (200-250g) were anaesthetized with an i.p. injection (60 mg/kg) of Somnotol®. The fundus, corpus, and antrum were dissected out, rinsed in sterile ice-cold saline, flash frozen in liquid nitrogen, and stored at -80°C until total RNA was extracted. The gastric mucosa was obtained by gently scraping the luminal surface of the stomach using a sterile glass slide. Total RNA was extracted immediately from the mucosa and striatum. The latter tissue has been shown to express moderate levels of A_1 receptor mRNA (Dixon et al., 1996) and was used as a positive control. Total RNA was extracted from tissues using Trizol® reagent (Invitrogen Corp. Carlsbad, CA) according to manufacturer's instructions. The total RNA concentration was determined by the following calculation: concentration (micrograms per milliliter) = $A_{260} \times 40\ \mu g/ml \times 100$ (dilution factor).

DNase I treatment, first strand cDNA synthesis and PCR

DNase I treatment was performed at room temperature in 1× first strand buffer [50 mM Tris-HCl (pH 8.3 at 25°C), 75 mM KCl, 3 mM $MgCl_2$] containing 1U DNase I/µg total RNA (Invitrogen), according to manufacturers' instructions. First strand cDNA was synthesized from 5 µg of DNase I-treated total RNA using Superscript II RNase H- Reverse Transcriptase (Invitrogen). A

sample containing autoclaved distilled water instead of total RNA was used as the negative control.

The PCR reaction mixture (50 µl) consisted of 2 µl cDNA in 1× PCR buffer [20 mM Tris-HCl (pH 8.4), and 50 mM KCl] containing 0.2 mM dNTP mix, 1.5 mM $MgCl_2$, 100 ng each of forward and reverse primer, and 1 U Platinum Taq DNA Polymerase (Invitrogen). A positive control sample containing striatal cDNA and a negative control from the first strand synthesis step were included for all experiments. The PCR was performed using the Robocycler Temperature cycler (Stratagene, La Jolla, CA). Thirty cycles of amplification were performed. Each cycle consisted of a 45-sec denaturation period at 94°C, a 1-min annealing period at 58°C, and a 1-min extension period at 72°C. PCR products were electrophoresed through a 2.5% agarose gel (w/v) containing 1× Tris acetate EDTA (TAE) buffer [40 mM Tris acetate and 1 mM EDTA (pH 8.5)] and ethidium bromide (0.5 µg/ml). Gels were run in 1× TAE buffer at 100 V for 45 min, and visualized and photographed under UV light using the Stratagene Eagle Eye II system (La Jolla, CA).

Cloning and sequencing of the mucosal A_1 receptor gene

The A_1 receptor RT-PCR product generated using mucosal tissue as the template was ligated into the pGEM-T vector (Promega, Madison, WI) and transformed into DHα-competent Escherichia coli cells (Invitrogen). Cells were grown in LB plates containing ampicillin (100 µg/ml), isopropyl β-D-thiogalactopyranoside (0.5 mM), and 5-bromo-4-chloro-3-indolyl-ß-D-galactoside (80 µg/ml). Plasmid DNA was purified using the QIAprep Miniprep kit (QIAGEN, Mississauga, ON) and sequenced at the Nucleic Acid Protein Services Unit using the T7 primer and SP6 primer. The gene sequence of the mucosal A_1 receptor was aligned with the published sequence

in the rat brain using the "University of Southern California (USC) Sequence Alignment Server" (http://www-hto.usc.edu/software/seqaln/seqaln-query.html) and submitted to the GenBank database at the National Center for Biotechnology Information.

Quantification of A_1 receptor gene expression by real-time RT-PCR

A two-step real-time RT-PCR assay was performed to quantify A_1 receptor gene expression in various regions of the rat stomach. For comparison, A_1 receptor gene expression was also measured in the rat striatum. Primers and probes were designed using the Primer Express Sequence Design software program (v. 1.0, Applied Biosystems, Foster City, CA). The reporter dye, 6-carboxyfluorescein (FAM) and the quencher dye, 6-carboxytetramethylrhodamine (TAMRA) were linked to the 5' and 3' ends of the A_1 receptor probe, respectively. The sequences of the forward primer, reverse primer and probe are 5'CGGTGACCCCCAGAAGTACTAC3', 5'GGGCAAAGAGGAAGAGGATGA3' and FAM-5'CAGCGACTTGGCGATCTTCAGCTCCT3'-TAMRA, which correspond to positions 963-984, 989-1014 and 1039-1059 bp of the rat brain A_1 receptor gene (accession #M64299), respectively. The primer and probes were synthesized by the Nucleic Acid Protein Services Unit at UBC and by Synthegen, LLC (Houston, TX), respectively.

RNA transcripts expressing the entire coding region of the A_1 receptor were used as the standard for quantification during real-time RT-PCR. The standard was synthesized using plasmids generated by the previous cloning experiments by *in vitro* transcription using the Riboprobe *in vitro* transcription kit and T7 RNA polymerase (Promega). The A_1 receptor RNA standard was DNase I-treated and purified, and its concentration was determined using the RiboGreen Reagent Quantitation kit (Molecular Probes, Eugene, OR), the FL600 Microplate

Fluorescence reader (Biotek Inc., Winooski, VT) and the KC4 Kineticalc Software (version 2.6, Biotek Inc.). RNA standards were then serially diluted to concentrations of 1×10^3 to 1×10^{12} copies/μl in RNase-free water, aliquoted, stored at -80°C, and thawed only once prior to use.

Two-step real-time RT- PCR

The level of A_1 receptor gene expression was measured in the whole fundus, corpus, antrum, the corporeal mucosa and corporeal muscle layers, the whole stomach mucosa, and the striatum (positive control). The methods for tissue extraction were described earlier. To obtain the corporeal mucosa and muscle tissue, the corporeal mucosa was gently scraped off the luminal surface of the corpus using a sterile glass slide. The remaining corporeal muscle tissue was flash frozen in liquid nitrogen and stored at -80°C until total RNA was isolated. Total RNA was extracted immediately from corporeal and whole stomach mucosa samples. The methods used for the isolation, quantification, and DNase I-treatment of total RNA were described earlier.

Reverse transcription: One microgram of DNase I-treated tissue RNA was reverse transcribed in a total volume of 10 μl containing 200 ng random hexamers, 20 U RNAguard RNase inhibitor, 1× first strand buffer, 10 mM DTT, 0.5 mM dNTP mix, and 100 U Superscript II RNase H- Reverse Transcriptase. At least 6 concentrations of the A_1 receptor RNA standard, ranging from 1×10^3 to 1×10^6 copies/μl, and a sample containing DNase I-treated RNase-free water in place of the template, were reverse-transcribed simultaneously. The reverse-transcribed RNA standards were used to construct the standard curve for the real-time RT-PCR assay, and the sample containing sterile water was used as the template for the negative control.

PCR: Each assay consisted of 6 standard curve samples, a negative control sample and unknown samples. All reactions were performed in triplicate. The PCR reaction mixture (25 μl)

consisted of 1× TaqMan buffer A, 200 μM of each dATP, dCTP, and dGTP, 400 μM dUTP, 0.01 U/μl AmpErase uracil-N-glycosylase (UNG), and 0.025 U/μl AmpliTaq Gold DNA polymerase from the TaqMan PCR Core Kit (Applied Biosystems, Foster City, CA). The reaction mixture also contained 0.5 μl of tissue cDNA, standard cDNA or negative control, 100 nM probe, 100 nM each of the forward and reverse primers, and 7.5 mM $MgCl_2$. The reaction was performed using the ABI Prism 7700 Sequence Detector (Applied Biosystems) with the following cycling parameters: 2-min hold at 50°C for UNG incubation, 10-min hold at 95°C for AmpliTaq Gold activation, followed by 40 cycles of amplification consisting of a 15-sec denaturation step at 95°C and 1-min anneal/extend period at 60°C.

Data collection and analysis: Data were collected during each PCR cycle and analyzed using the Sequence Detection Software (v. 1.6.3, Applied Biosystems). An amplification plot showing normalized reporter emissions vs. cycle number was generated (see Fig. 8B). The threshold cycle (C_T), the cycle where an increase in fluorescence is associated with exponential growth, was determined by the software using the fluorescence emitted during the first 15 cycles. A standard curve of C_T vs. Log (initial A_1 receptor standard concentrations) was generated (see Fig. 8C). The initial concentration of each unknown sample was determined by interpolation using the C_T value determined by the assay. The correlation coefficient of each standard curve was > 0.95, and the C_T of the no template controls exceeded 40 cycles in every assay, indicating the absence of DNA contamination. Results were expressed as copies of mRNA per μg total RNA. Statistical significance was determined using GraphPad Prism and the two-tailed unpaired Student's t-test, where $P < 0.05$ was considered significant.

Results

Effect of adenosine agonists on IRG release

To examine the adenosine receptor(s) involved in the regulation of IRG release, the effect of the A_1- (CPA), A_{2A}- (CGS 21680), and A_3- (IB-MECA) selective agonists was examined since specific agonists for individual receptor subtypes are unavailable. Basal IRG release (periods 1 to 3) was shown to remain relatively constant in experiments examining the effect of 0.1 μM CPA (194±42 to 194±47 pg/min), 0.1 μM CGS 21680 (123±21 to 124±19 pg/min) and 0.1 μM IB-MECA (185±24 to 201±24 pg/min) on IRG release (Fig. 2). Fig. 2A demonstrates that the administration of 0.1 μM CPA caused a significant inhibition of IRG release starting at period 5 and continued throughout the drug perfusion period. Upon the cessation of CPA perfusion, IRG release returned to basal levels. The same concentration of CGS 21680 and IB-MECA did not alter basal IRG release (Fig. 2B and 2C). The effect of various concentrations of these analogs on IRG release was also examined. The results are expressed as percent inhibition and summarized in Fig. 3. CPA was shown to suppress IRG release concentration-dependently. CPA caused significant inhibition of IRG release starting at a concentration of 0.001 μM (12±5%), and maximum suppression of IRG release was reached at 1 μM (43±5%). The empirical EC_{50} of CPA in inhibiting IRG release was estimated to be 0.067 μM, with a 95% confidence interval between 0.014 and 0.325 μM. CGS 21680 (0.001 to 0.1 μM) did not alter IRG release. However, significant inhibition (14±5%) was observed when 1 μM CGS21680 was perfused into the stomach. All concentrations of IB-MECA examined (0.001 μM to 1 μM) did not alter IRG release.

JPET Fast Forward. Published on March 24, 2004 as DOI: 10.1124/jpet.104.066654
This article has not been copyedited and formatted. The final version may differ from this version.

Effect of DPCPX and DMPX on IRG release

We have previously demonstrated that the endogenous compound, adenosine, also inhibited IRG release concentration-dependently (Kwok et al., 1990). To test if this inhibitory action is mediated by A_1 receptors, the effect of the antagonists, DPCPX (A_1-selective) and DMPX (A_2-selective) on basal and adenosine-stimulated IRG release was examined. When DPCPX or DMPX was perfused alone into the stomach for 20 min (periods 4 to 7), no significant changes in IRG release were apparent; the percent change of IRG in the presence of DPCPX or DMPX alone were 7±4% (n=6) and 0±4% (n=6), respectively. Fig. 4A shows that adenosine (10 μM) significantly inhibited IRG release when it was administered alone for 15 min. To test the effect of DPCPX and DMPX on adenosine-induced IRG release, the antagonist was perfused 5 min before the concomitant perfusion of both adenosine and antagonist for 15 min. In the presence of DPCPX, the inhibitory effect of adenosine was completely abolished (Fig. 4B). Adenosine-induced inhibition of IRG release was not altered by the concomitant perfusion with DMPX (Fig. 4C).

Cellular localization and distribution of A_1R-IR

Since the results of the perfusion studies suggest that the A_1 receptor is involved in the inhibition of IRG release, immunohistochemistry experiments were performed to determine the cellular localization and distribution of A_1 receptors in the rat stomach. The distribution of A_1R-IR was similar in the gastric antrum and corpus (Fig. 5). Abundant A_1R-IR was observed along the basal region of the antral mucosa (Fig. 5A). When viewed under high magnification, A_1R-IR was found to be intense and punctuate (Fig. 5B). A_1R-IR was dispersed uniformly throughout the corporeal mucosa, except at the tips of the mucosa (Fig. 5C and 5D). In both the corpus and

antrum, A_1R-IR was also observed on cell bodies and nerve fibers of the myenteric plexus, nerve fibers of the circular muscle layer, longitudinal muscle layer, muscularis mucosae and submucosal plexus, and blood vessels (Fig. 5E and 5F). No A_1R-IR was observed when tissue sections were incubated with the immunoneutralized A_1 receptor antibody (Fig. 5G) or with the Cy3-conjugated secondary antibody alone (Fig. 5H).

To examine whether A_1R-IR is localized on gastrin-secreting G-cells, double staining experiments were performed. Abundant gastrin-IR was observed along the base of the antral mucosa (Fig. 6B). Double staining revealed that all gastrin-IR cells examined contained A_1R-IR (Fig. 6C). In addition, A_1R-IR (Fig. 6A) appeared most intense in mucosal cells expressing gastrin-IR. Although all gastrin-IR cells expressed A_1R-IR, approximately 28±2% of A_1R-IR cells of the antral mucosa expressed gastrin-IR.

To determine if A_1R-IR was also localized on somatostatin-secreting D-cells of the antral and corporeal mucosa, double staining experiments were also performed with antibody against somatostatin. Intense and abundant somatostatin-IR was observed in the antral and corporeal mucosa while sparse somatostatin-IR was observed throughout the rest of the tissue. Double staining with A_1R-IR revealed that some somatostatin-IR cells of the antral and corporeal mucosa also expressed A_1R-IR (Fig. 6D-I). In somatostatin-IR cells of the corpus, A_1R-IR appeared most intense at the end of the cell processes (Fig. 6G-I and 6J-L). Quantification of A_1R-IR revealed that all somatostatin-IR cells of the corporeal mucosa expressed A_1R-IR, while approximately 24±2% of somatostatin-IR cells of the antrum expressed A_1R-IR. The present study also demonstrates that 8.5±0.6% of A_1R-IR cells of the antral mucosa expressed somatostatin-IR. A_1R-IR was shown not to co-localize with somatostatin-IR in other regions of the antrum and corpus, including the myenteric plexus and muscle layers.

Double staining experiments were also performed to localize A_1R-IR in relation to the immunoreactivity of H^+K^+-ATPase β (parietal cell marker), VWF (endothelial cell marker), and PGP 9.5 (neuronal marker). Results show that A_1R-IR was not co-localized with H^+K^+-ATPase β-IR (Fig. 7 A-C). However, A_1R-IR was co-localized with VWF-IR and PGP 9.5-IR throughout the corpus and antrum (Fig. 7 D-I). A_1R-IR was expressed with VWF-IR in the muscle layers, myenteric and submucosal plexi (Fig. 7D-F), and with PGP 9.5-IR in cell bodies and nerve fibers of the myenteric plexus, nerve fibers of the submucosal plexus, circular and longitudinal muscle layers and muscularis mucosae (Fig. 7G-I).

Regional distribution, structure, and abundance of adenosine A_1 receptor mRNA

The expression of A_1 receptor mRNA was detected in all gastric regions examined, including the fundus, corpus, antrum, and mucosa. Only one RT-PCR amplicon of the expected size (1086 bp) was generated for all tissues, including the striatum, which was used as the positive control (Fig. 8A). Cloning and sequencing of the mucosal RT-PCR amplicon demonstrated that the coding region of the gastric mucosal A_1 receptor (submitted to GenBank; accession number: AF042079) was identical to the published sequence in the rat brain (Mahan et al., 1991) (accession number: M64299).

The real-time RT-PCR assay developed to quantify A_1 receptor gene expression in gastric tissues was shown to measure a 7 log range of A_1 receptor RNA concentrations. A representative amplification plot generated by the A_1 receptor real-time RT-PCR assay is shown on Fig. 8B. When a high concentration of A_1 receptor RNA standard (1×10^9 copies/μl) was used as the template, the reaction was affected by limiting reagents by cycle 22, and entered the plateau phase at cycle 26 (Fig. 8B). The standard curve generated by plotting the threshold cycle

(C_T) against the Log(A_1 receptor RNA standard concentration) is shown to be linear with an R value of 0.99 (Fig. 8C). Quantification of A_1 receptor gene expression using this assay demonstrated that the A_1 receptor mRNA level was highest in the corporeal muscle and lowest in the corporeal mucosa (Fig. 8D). A_1 receptor mRNA expression did not differ significantly among the corpus, antrum, and whole stomach mucosa. The fundic A_1 mRNA level was lower than those in the corpus, but not different from those in the antrum and mucosa. The striatal A_1 receptor mRNA level was at least 2-fold greater than levels measured in any gastric region examined. The striatum contained approximately 8.5×10^5 copies of A_1 receptor mRNA/μg total RNA, while the highest level measured in the stomach (corpus muscle) contained approximately 4.6×10^5 copies of A_1 receptor mRNA/μg total RNA.

Discussion

Adenosine has been shown to regulate gastric acid secretion and to protect the stomach against ulcer formation. In rats, adenosine inhibits gastric acid secretion, but does not act directly on the parietal cells to elicit this effect. Our laboratory has demonstrated that adenosine may mediate this inhibitory action by suppressing the release of gastrin (Kwok et al., 1990). Results of the present study show that CPA, the A_1 receptor-selective agonist (Williams et al., 1986), significantly inhibited IRG release starting at a concentration of 0.001 μM, and maximally inhibited IRG release at 1 μM. Although the A_{2A} receptor-selective agonist, CGS 21680, did not alter IRG release at lower concentrations, this compound did inhibit IRG release significantly at 1 μM. The percent inhibition of IRG release elicited by 1 μM CGS 21680 was similar to that produced by 0.001 μM CPA. Thus, the inhibitory effect of CGS 21680 is considerably weaker than that of CPA. The A_3 receptor-selective agonist, IB-MECA, did not alter IRG release. The potent inhibitory effect of CPA on IRG release may, therefore, suggest that the A_1 receptor subtype is likely involved in modulating IRG release. This proposal was further supported by the observation that the inhibitory effect of the endogenous compound, adenosine, on IRG release was completely abolished by the A_1 receptor-selective antagonist, DPCPX (Lohse et al., 1987), but not by the A_2 receptor-selective antagonist, DMPX (Seale et al., 1988). DPCPX exhibits a 700-fold preference for the A_1 receptor over the A_2 receptor (Bruns et al., 1987), while DMPX exhibits a 4-fold preference for the A_2 receptor over the A_1 receptor (Seale et al., 1988). At 1 μM, DPCPX and DMPX have been shown to completely abolish A_1 and A_{2A} receptor-mediated actions, respectively (Lohse et al., 1987; Seale et al., 1988). The present study also examined the possible site of action of the adenosine A_1 receptor-mediated

inhibitory action on IRG release by examining the immunohistochemical localization of the A_1 receptor.

A_1R-IR was expressed on all gastrin-IR G-cells examined, suggesting that adenosine may act directly on G-cells to inhibit IRG release. This proposal agrees well with studies showing that adenosine inhibited the release of gastrin in rat preparations containing G-cells (DeSchryver-Kecskemeti et al., 1981; Harty and Franklin, 1984) and in primary cultures of canine G-cells (Schepp et al., 1990). In these studies, the adenosine-induced inhibition was sensitive to blockade by theophylline and 8-phenyltheophylline (DeSchryver-Kecskemeti et al., 1981; Schepp et al., 1990). Xanthine derivatives such as theophylline, 8-phenyltheophylline and caffeine are non-selective antagonists of the adenosine receptors, and may block adenosine receptor-mediated responses (Ralevic and Burnstock, 1998). The present study further shows that the inhibitory effect of adenosine can be abolished by the A_1 receptor-selective antagonist, DPCPX, thus, confirming the involvement of extracellular adenosine receptors.

A_1R-IR was co-localized with somatostatin-IR in cells of the antral and corporeal mucosa, suggesting that A_1 receptors may be expressed on D-cells. Somatostatin was shown to inhibit IRG release (Saffouri et al., 1980). Thus, adenosine may inhibit IRG release by modulating the release of somatostatin. Adenosine has been demonstrated to regulate somatostatin-like immunoreactivity (SLI) release in the isolated vascularly perfused rat stomach (Kwok et al., 1990). Activation of adenosine A_1 and A_{2A} receptors may lead to inhibition and stimulation of SLI release, respectively (Yip and Kwok, 2004). However, it is doubtful that adenosine inhibits IRG release indirectly by modulating SLI release. Activation of A_1 receptors inhibits SLI release, which would lead to an increase, rather than a decrease in IRG release. Activation of A_{2A} receptors stimulates SLI release, which may subsequently inhibit IRG release. However, the

JPET Fast Forward. Published on March 24, 2004 as DOI: 10.1124/jpet.104.066654
This article has not been copyedited and formatted. The final version may differ from this version.

adenosine-induced inhibition of IRG release was completely abolished by DPCPX and not altered by DMPX, suggesting that A_{2A} receptor-induced SLI release is not involved in suppressing IRG release. Previous studies have shown that adenosine A_{2A} receptors are expressed on D-cells, indicating that adenosine may act directly on these cells to stimulate somatostatin release (Yip and Kwok, 2004). The co-localization of A_1R-IR with somatostatin-IR observed in the present study suggests that adenosine may also act directly on D-cells to inhibit somatostatin release. Adenosine may, therefore, play a dual role in the regulation of somatostatin release. It may inhibit and stimulate somatostatin release via activation of A_1 and A_{2A} receptors on D-cells, respectively.

A_1R-IR was not co-localized with H^+K^+-ATPase β-IR, indicating the absence of A_1 receptors on parietal cells. The lack of A_1R-IR on parietal cells suggests that adenosine does not act directly on these cells to inhibit acid secretion. This finding confirms previous studies demonstrating the inability of N^6(-)-phenylisopropyladenosine to alter carbachol- and histamine-stimulated acid secretion in rat parietal cell preparations (Puurunen et al., 1987).

A_1R-IR was also expressed on vasculature and nerve fibers throughout the stomach, as indicated by its co-localization with VWF-IR and PGP 9.5-IR, respectively. The vascular localization of these receptors fits well with previously observed A_1 receptor-mediated vascular actions (Tabrizchi and Bedi, 2001). Abundant A_1R-IR was present on nerve fibers of the myenteric and submucosal plexi. These localizations are consistent with studies demonstrating the involvement of A_1 receptors in the inhibition of neurotransmitter release from myenteric (Palmer et al., 1987) and submucosal (Barajas-Lopez et al., 1991) neurons. A_1 receptors have been implicated in the inhibition of acetylcholine and noradrenaline release (Barajas-Lopez et al., 1991; Nitahara et al., 1995; Ribeiro et al., 1996). Since both neurotransmitters can alter IRG

release (Koop et al., 1982; Koop et al., 1983), it is conceivable that the effect of adenosine on IRG release is secondary to its effect on adrenergic and cholinergic neurotransmission. Although this possibility was not determined, the localization of A_1R-IR on all gastrin-IR cells examined suggests that adenosine may inhibit IRG release, at least in part, by acting directly on G-cells.

The structure of the gastric A_1 receptor was also examined in the present study. Two distinct A_1 receptor mRNA transcripts have been detected by Northern blot analysis in the rat stomach (Mahan et al., 1991; Reppert et al., 1991). However, when RT-PCR experiments were performed using primers that span the entire coding region of the A_1 receptor gene, only one amplicon was produced. Thus, alternative splicing is unlikely to occur within the coding region of the gastric A_1 receptor gene. In humans, two promoters drive the synthesis of two distinct A_1 receptor transcripts that differ in the 5'-untranslated region (Ren and Stiles, 1995). Thus, the two A_1 receptor transcripts previously detected in the rat stomach may be generated by separate promoters or alternative splicing of the 5'-untranslated region. The present cloning and sequencing experiments reveal that the coding region of the gastric A_1 receptor was identical to the rat brain sequence (Mahan et al., 1991), indicating that only one form of the A_1 receptor, identical to the rat brain receptor, exists in the stomach.

Results also show that A_1 receptor gene expression was expressed in all functionally and morphologically distinct regions of the stomach. Real-time RT-PCR was used to measure the level of A_1 receptor gene expression in various gastric regions. This assay was shown to accurately quantify over a 7 log range of concentrations and less than 500 copies of A_1 receptor RNA/μg total tissue RNA (~ 25 copies per reaction tube). In agreement with previous studies (Dixon et al., 1996), results demonstrate that A_1 receptor gene expression was higher in the striatum than the stomach. The striatal A_1 receptor mRNA level was at least 2-fold higher than

any gastric region examined. Among the gastric tissues, the A_1 receptor mRNA level was lowest in the corporeal mucosa and highest in the corporeal muscle. These findings correspond well with results of the immunohistochemistry studies. In the corpus, A_1R-IR was found on some mucosal cells, but the majority was localized on nerve fibers and vasculature of the muscle layers and myenteric plexus. The abundant A_1R-IR observed at the base of the antral mucosa and the moderate A_1R-IR observed throughout the corporeal mucosa is also consistent with the higher level of A_1 receptor mRNA measured in the whole stomach mucosa compared to the corporeal mucosa.

In conclusion, the results of this study suggest that, in the rat stomach, adenosine may mediate its inhibitory action on IRG release, at least in part, by acting on A_1 receptors of G-cells. The inhibition of IRG release may subsequently lead to a decrease in gastric acid secretion. The gastric A_1 receptor was found to be structurally identical to that in the rat brain, and was expressed on various cells throughout the stomach, including the G-cells. The gene expression of the A_1 receptor was extremely low in all gastric tissues examined, although it was easily quantified by the sensitive real-time RT-PCR assay developed in the present study.

References

Barajas-Lopez C, Surprenant A and North RA (1991) Adenosine A1 and A2 receptors mediate presynaptic inhibition and postsynaptic excitation in guinea pig submucosal neurons. *J Pharmacol Exp Ther* **258**:490-495.

Bruns RF, Fergus JH, Badger EW, Bristol JA, Santay LA, Hartman JD, Hays SJ and Huang CC (1987) Binding of the A1-selective adenosine antagonist 8-cyclopentyl-1,3-dipropylxanthine to rat brain membranes. *Naunyn Schmiedebergs Arch Pharmacol* **335**:59-63.

Carruthers AM, Sellers LA, Jenkins DW, Jarvie EM, Feniuk W and Humphrey PP (2001) Adenosine A(1) receptor-mediated inhibition of protein kinase A-induced calcitonin gene-related peptide release from rat trigeminal neurons. *Mol Pharmacol* **59**:1533-1541.

DeSchryver-Kecskemeti K, Greider MH, Rieders ER, Komyati SE and McGuigan JE (1981) In vitro gastrin secretion by rat antrum: effects of neurotransmitter agonists, antagonists, and modulators of secretion. *Lab Invest* **44**:158-163.

Dixon AK, Gubitz AK, Sirinathsinghji DJ, Richardson PJ and Freeman TC (1996) Tissue distribution of adenosine receptor mRNAs in the rat. *Br J Pharmacol* **118**:1461-1468.

Fredholm BB, AP IJ, Jacobson KA, Klotz KN and Linden J (2001) International Union of Pharmacology. XXV. Nomenclature and classification of adenosine receptors. *Pharmacol Rev* **53**:527-552.

Fujimiya M and Kwok YN (1997) Effect of carbachol on vascular and luminal release of immunoreactive gastrin from isolated perfused rat duodenum. *Dig Dis Sci* **42**:634-639.

Geiger JD and Glavin GB (1985) Adenosine receptor activation in brain reduces stress-induced ulcer formation. *Eur J Pharmacol* **115**:185-190.

Gerber JG, Nies AS and Payne NA (1985) Adenosine receptors on canine parietal cells modulate gastric acid secretion to histamine. *J Pharmacol Exp Ther* **233**:623-627.

Gerber JG and Payne NA (1988) Endogenous adenosine modulates gastric acid secretion to histamine in canine parietal cells. *J Pharmacol Exp Ther* **244**:190-194.

Glavin GB, Westerberg VS and Geiger JD (1987) Modulation of gastric acid secretion by adenosine in conscious rats. *Can J Physiol Pharmacol* **65**:1182-1185.

Harty RF and Franklin PA (1984) Effects of exogenous and endogenous adenosine on gastrin release from rat antral mucosa. *Gastroenterology* **86**:1107.

Heldsinger AA, Vinik AI and Fox IH (1986) Inhibition of guinea-pig oxyntic cell function by adenosine and prostaglandins. *J Pharmacol Exp Ther* **237**:351-356.

Jaffe B and Walsh JH (1978) Gastrin and related peptides, in *Methods of Hormone Radioimmunoassay* (Jaffe bM and Behrman HR eds) pp 455-477, Academic Press, New York.

Koop H, Behrens I, Bothe E, Koschwitz H, McIntosh CH, Pederson RA, Arnold R and Creutzfeldt W (1983) Adrenergic control of rat gastric somatostatin and gastrin release. *Scand J Gastroenterol* **18**:65-71.

Koop H, Behrens I, Bothe E, McIntosh CH, Pederson RA, Arnold R and Creutzfeldt W (1982) Adrenergic and cholinergic interactions in rat gastric somatostatin and gastrin release. *Digestion* **25**:96-102.

Kwok YN, McIntosh C and Brown J (1990) Augmentation of release of gastric somatostatin-like immunoreactivity by adenosine, adenosine triphosphate and their analogs. *J Pharmacol Exp Ther* **255**:781-788.

Lohse MJ, Klotz KN, Lindenborn-Fotinos J, Reddington M, Schwabe U and Olsson RA (1987) 8-Cyclopentyl-1,3-dipropylxanthine (DPCPX)--a selective high affinity antagonist radioligand for A1 adenosine receptors. *Naunyn Schmiedebergs Arch Pharmacol* **336**:204-210.

Mahan LC, McVittie LD, Smyk-Randall EM, Nakata H, Monsma FJ, Jr., Gerfen CR and Sibley DR (1991) Cloning and expression of an A1 adenosine receptor from rat brain. *Mol Pharmacol* **40**:1-7.

Nitahara K, Kittel A, Liang SD and Vizi ES (1995) A1-receptor-mediated effect of adenosine on the release of acetylcholine from the myenteric plexus: role and localization of ecto-ATPase and 5'-nucleotidase. *Neuroscience* **67**:159-168.

Palmer JM, Wood JD and Zafirov DH (1987) Purinergic inhibition in the small intestinal myenteric plexus of the guinea-pig. *J Physiol* **387**:357-369.

Pederson RA, Kwok YN, Buchan AM, McIntosh CH and Brown JC (1984) Gastrin release from isolated perfused rat stomach after vagotomy. *Am J Physiol* **247**:G248-252.

Puurunen J, Ruoff HJ and Schwabe U (1987) Lack of direct effect of adenosine on the parietal cell function in the rat. *Pharmacol Toxicol* **60**:315-317.

Ralevic V and Burnstock G (1998) Receptors for purines and pyrimidines. *Pharmacol Rev* **50**:413-492.

Ren H and Stiles GL (1995) Separate promoters in the human A1 adenosine receptor gene direct the synthesis of distinct messenger RNAs that regulate receptor abundance. *Mol Pharmacol* **48**:975-980.

Reppert SM, Weaver DR, Stehle JH and Rivkees SA (1991) Molecular cloning and characterization of a rat A1-adenosine receptor that is widely expressed in brain and spinal cord. *Mol Endocrinol* **5**:1037-1048.

Ribeiro JA, Cunha RA, Correia-de-Sa P and Sebastiao AM (1996) Purinergic regulation of acetylcholine release. *Prog Brain Res* **109**:231-241.

Saffouri B, Weir GC, Bitar KN and Makhlouf GM (1980) Gastrin and somatostatin secretion by perfused rat stomach: functional linkage of antral peptides. *Am J Physiol* **238**:G495-501.

Sajjadi FG, Boyle DL, Domingo RC and Firestein GS (1996) cDNA cloning and characterization of A3i, an alternatively spliced rat A3 adenosine receptor variant. *FEBS Lett* **382**:125-129.

Sambrook J, Fritsch EF and Maniatis T (1989) Detection and analysis of proteins expressed from cloned genes, in *Molecular cloning: a laboratory manual* (Nolan C ed) pp 18.11-18.88, Cold Spring Harbor Laboratory Press, Plainview.

Schepp W, Soll AH and Walsh JH (1990) Dual modulation by adenosine of gastrin release from canine G-cells in primary culture. *Am J Physiol* **259**:G556-563.

Seale TW, Abla KA, Shamim MT, Carney JM and Daly JW (1988) 3,7-Dimethyl-1-propargylxanthine: a potent and selective in vivo antagonist of adenosine analogs. *Life Sci* **43**:1671-1684.

Tabrizchi R and Bedi S (2001) Pharmacology of adenosine receptors in the vasculature. *Pharmacol Ther* **91**:133-147.

Westerberg VS and Geiger JD (1987) Central effects of adenosine analogs on stress-induced gastric ulcer formation. *Life Sci* **41**:2201-2205.

Westerberg VS and Geiger JD (1989) Adenosine analogs inhibit gastric acid secretion. *Eur J Pharmacol* **160**:275-281.

Williams M, Braunwalder A and Erickson TJ (1986) Evaluation of the binding of the A-1 selective adenosine radioligand, cyclopentyladenosine (CPA), to rat brain tissue. *Naunyn Schmiedebergs Arch Pharmacol* **332**:179-183.

Yip L and Kwok YN (2004) Role of adenosine A2A receptor in the regulation of gastric somatostatin release. *J Pharmacol Exp Ther* **(in press)**.

Yip L, Kwok YN and Buchan AM (2003) Cellular localization and distribution of neurokinin-1 receptors in the rat stomach. *Auton Neurosci* **104**:95-108.

Footnotes:

This work was supported by the Canadian Apoptosis Research Foundation Society, Canada Foundation for Innovation, Wah Sheung Fund and the former BCHRF. Linda Yip was supported by the Cordula and Gunter Paetzold Fellowship and the University of British Columbia Graduate Fellowship.

A portion of this work was included in Linda Yip's Ph.D. dissertation entitled: Adenosine A_1 and A_{2A} Receptors in the Rat Stomach: Biological Actions, Cellular Localization, Structure, and Gene Expression.

Citation of meeting abstracts where part of this work was previously presented:

Yip L and Kwok Y (2002) Gastric A_1 and A_{2A} receptors: cellular localization, gene sequence and gene expression levels. *Drug Dev Res* 56:551.

Yip L, Leung CH and Kwok YN (2003) Cellular localization of adenosine A_1 and A_{2A} receptors in the rat stomach. *FASEB J* 17:A40.

Please send reprints requests to: Yin Nam Kwok Ph.D., Department of Physiology, University of British Columbia, 2146 Health Sciences Mall, Vancouver, BC. Canada. V6T 1Z3. Tel: 604-822-6228, Fax: 604-822-6048, Email: kynkwok@interchange.ubc.ca

Figure Legends

Fig. 1 Western blot analysis of adenosine A_1 receptors in rat tissues. Two immunogenic bands at 40.5 kDa and 67 kDa were detected in protein extracts of the fundus, corpus, antrum and brain.

Fig. 2 Effect of CPA, CGS 21680 and IB-MECA on basal IRG release. Results are expressed as IRG release (%) as described in the Methods section. Each column represents the mean ± SEM; $n \geq 5$. *$P < 0.05$ when compared with period 3 of respective experiments using repeated measures analysis of variance followed by Dunnett's multiple comparison test.

Fig. 3 Effect of various concentrations of CPA, CGS 21680 and IB-MECA on IRG release. Results are expressed as percentage (%) inhibition and calculated as described in the Methods section. Each column represents the mean ± SEM of at least 5 experiments. *$P < 0.05$ and ***$P < 0.001$ when comparing the mean IRG release (pg/min) in the presence of drug during periods 4-7 with that of periods 1-3 (basal release).

Fig. 4 Effect of DPCPX and DMPX on adenosine-induced inhibition of IRG release. A: Effect of adenosine (ADO) on basal IRG release; B: Effect of DPCPX on ADO-induced inhibition of IRG release; C: Effect of DMPX on ADO-induced inhibition of IRG release. Each column represents the mean ± SEM; $n \geq 5$; *$P < 0.05$ and ***$P < 0.001$ when compared with period 3 of respective experiments.

Fig. 5 Confocal images showing A_1R-IR in the antrum and corpus of the rat stomach. A: A_1R-IR cell in the antral mucosa (arrows). B: The boxed area in panel A, viewed under high magnification. C: A_1R-IR cells in the corporeal mucosa (arrows). D: A_1R-IR cells in the corporeal mucosa, viewed under high magnification. E: A_1R-IR on blood vessels (arrow; BV) and nerve fibers (arrowheads) in the submucosal plexus (SMP) of the corpus. F: A_1R-IR on nerve fibers and cell bodies of the myenteric plexus (arrowhead), and on nerve fibers of the circular (arrows; CM) and longitudinal muscle (arrows; LM) of the antrum. G: Confocal image showing the lack of A_1R-IR in the antral mucosa; section was incubated with the immunoneutralized A_1 receptor antibody. H: Confocal image showing the lack of A_1R-IR in the corporeal muscle; section was incubated with the secondary antibody, donkey anti-rabbit IgG conjugated to cyanine Cy3 (1:2,000) alone. (z-step = 1.0 μm and scale bar = 25 μm for all images).

Fig. 6 Double staining of A_1R-IR with gastrin-IR and somatostatin-IR in the rat stomach. A-C: Co-localization of A_1R-IR (A) with gastrin-IR (B) in the antral mucosa. D-F: Co-localization of A_1R-IR (D) and somatostatin-IR (E) in the antral mucosa. G-I: Co-localization of A_1R-IR (G) and somatostatin-IR (H) in the corporeal mucosa. J-L: High magnification image showing the co-localization of A_1R-IR (J) and somatostatin-IR (K) in a single cell of the corporeal mucosa (L). Cells expressing both A_1R-IR (red) and gastric peptide-IR (green) are indicated by arrows and look yellow in the merged panel (C, F, I & L). A_1R-IR cells that do not contain gastrin-IR or somatostatin-IR are indicated by arrowheads. (z-step = 1.0 μm and scale bar = 25 μm for all images).

Fig. 7 Double staining of A_1R-IR with H^+K^+-ATPase β, VWF, and PGP 9.5-IR in the rat corpus. A-C: A_1R-IR (A) with H^+K^+-ATPase β-IR (B) in the corporeal mucosa. D-F: Co-localization of A_1R-IR (D) and VWF-IR (E) on a blood vessel in the circular muscle. G-I: Co-localization of A_1R-IR (G) with PGP 9.5-IR (H) on nerve fibers and cell bodies of the myenteric plexus (arrowhead) and nerve fibers of the circular muscle (arrows). Cells expressing both immunoreactivities look yellow in the merged panels (F & I). (z-step = 1.0 μm and scale bar = 25 μm for all images).

Fig. 8 Distribution and abundance of A_1 receptor mRNA in the rat stomach. A: Results of RT-PCR performed using primers which span the entire coding region of the A_1 receptor gene. A single amplicon was generated using cDNA from the fundus (lane 2), corpus (lane 3), antrum (lane 4) mucosa (lane 5) and striatum (positive control; lane 1) as the template. Ladder = 100 bp ladder. B: Amplification plots generated by the A_1 receptor real-time RT-PCR assay using various concentrations of A_1 receptor RNA as the standard. The amplification plots (from left to right) were generated using 1×10^9, 1×10^8, 1×10^7, 1×10^6, 1×10^5, 1×10^4, and 1×10^3 copies of A_1 receptor RNA. C: The corresponding standard curve generated by the amplification plots shown in B. Correlation coefficient = 0.99. D: A_1 receptor gene expression levels measured in various regions of the rat stomach using real-time RT-PCR. Each bar represents the mean ± SEM of at least 4 animals. A_1 receptor gene expression was also quantified in the striatum and found to contain 850 ± 55 thousand copies of A_1 receptor mRNA/μg total RNA.

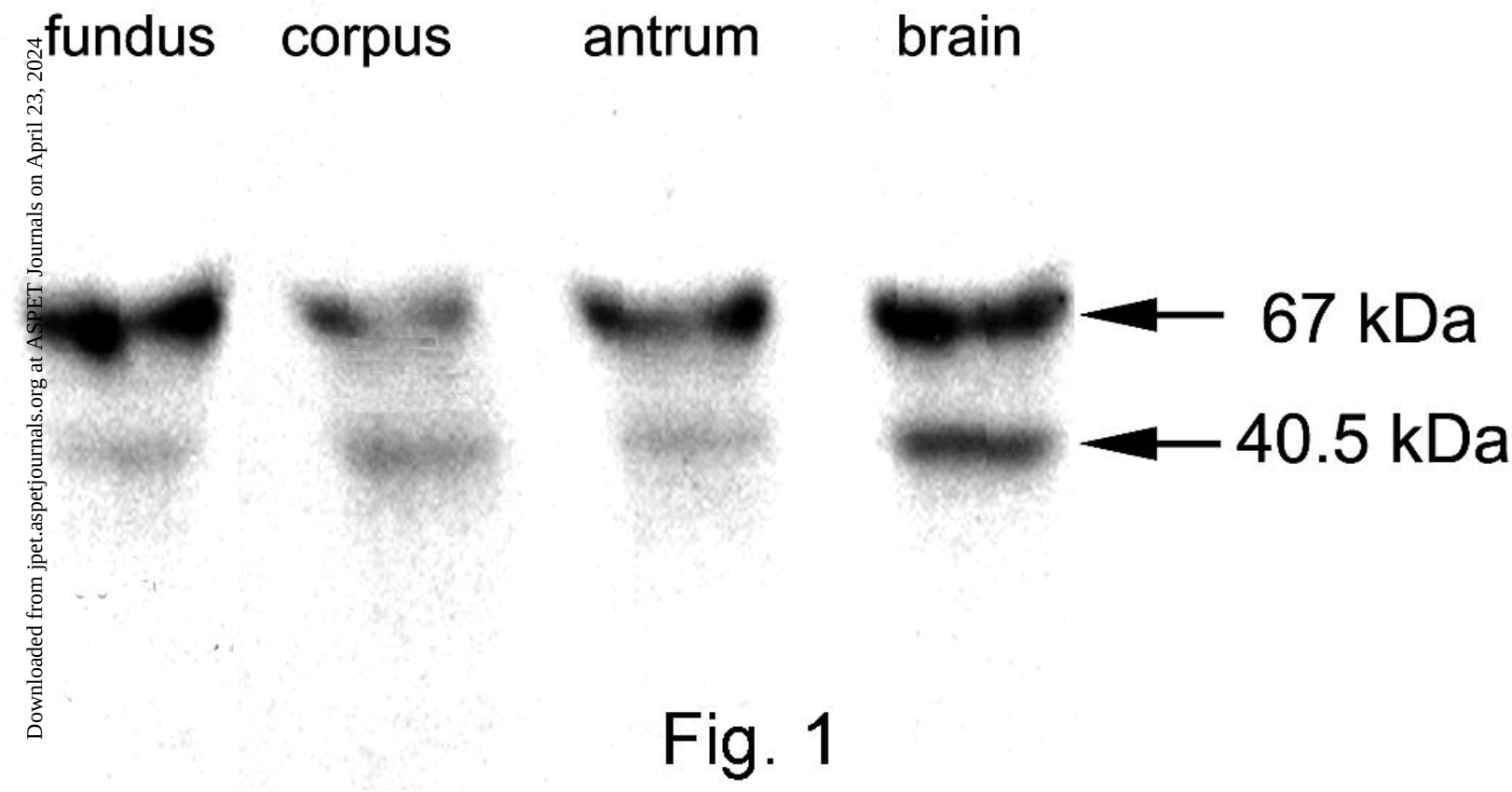

Fig. 1

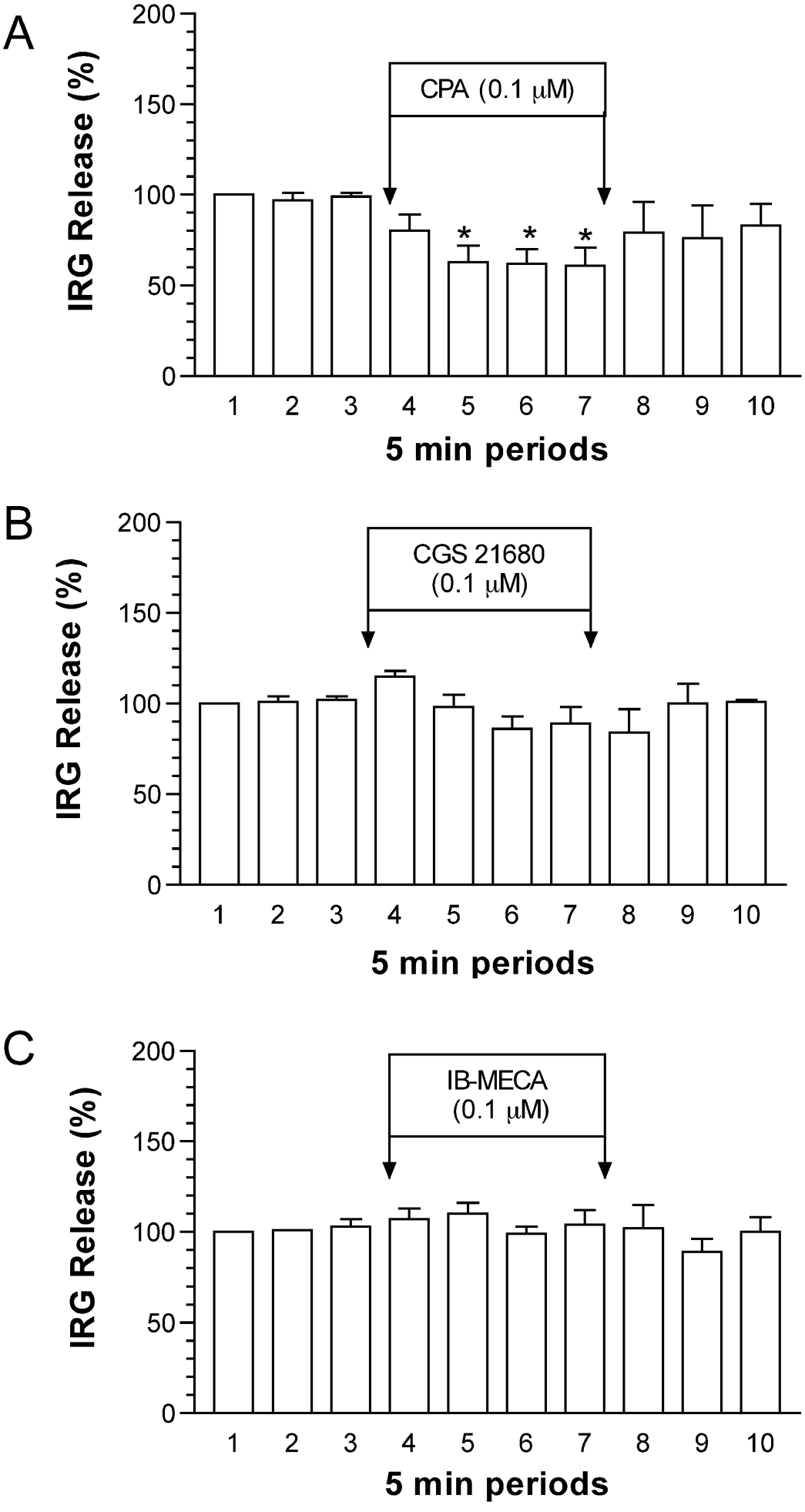

Fig. 2

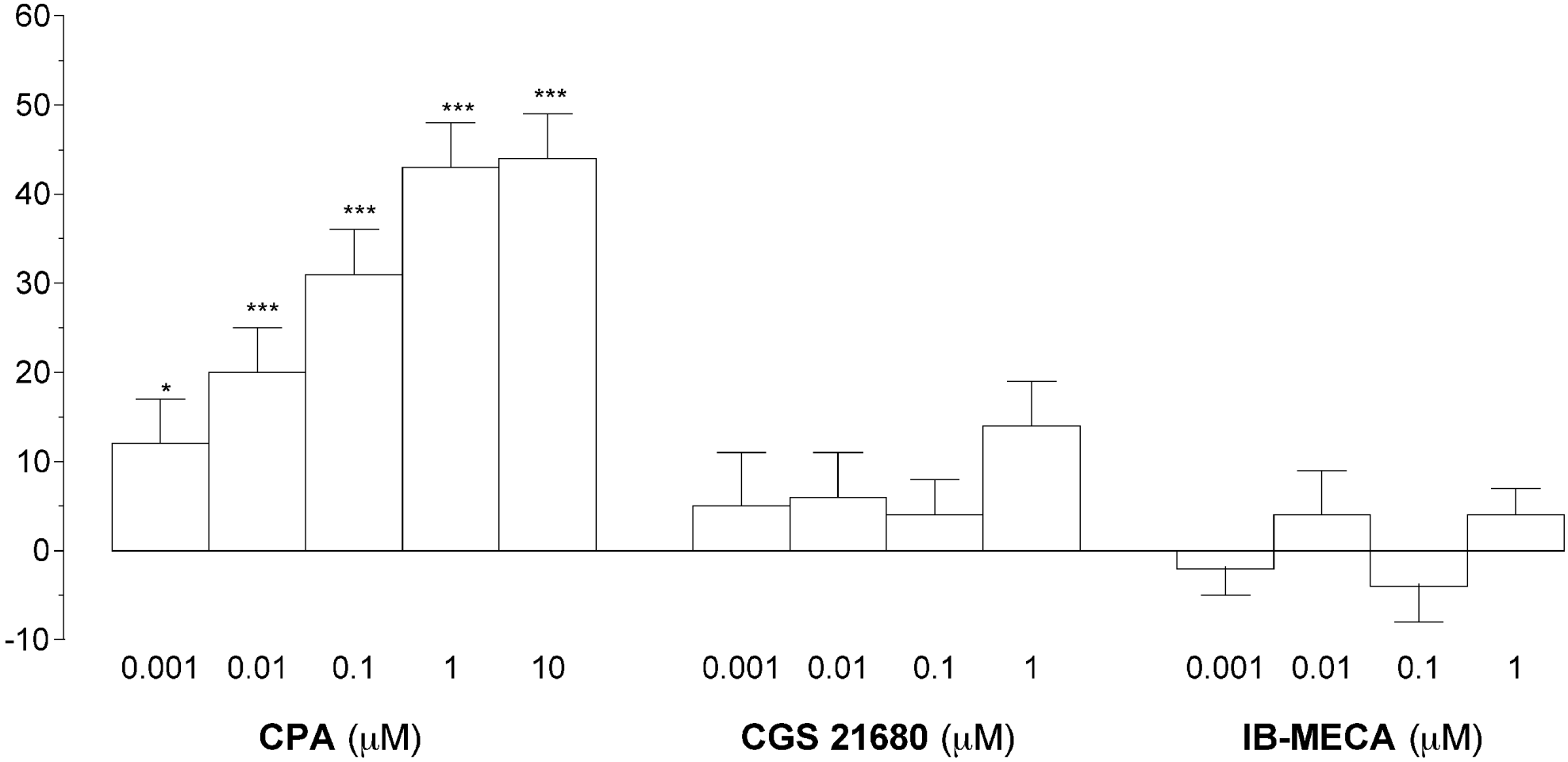

RG Release (% inhibition)

Fig. 3

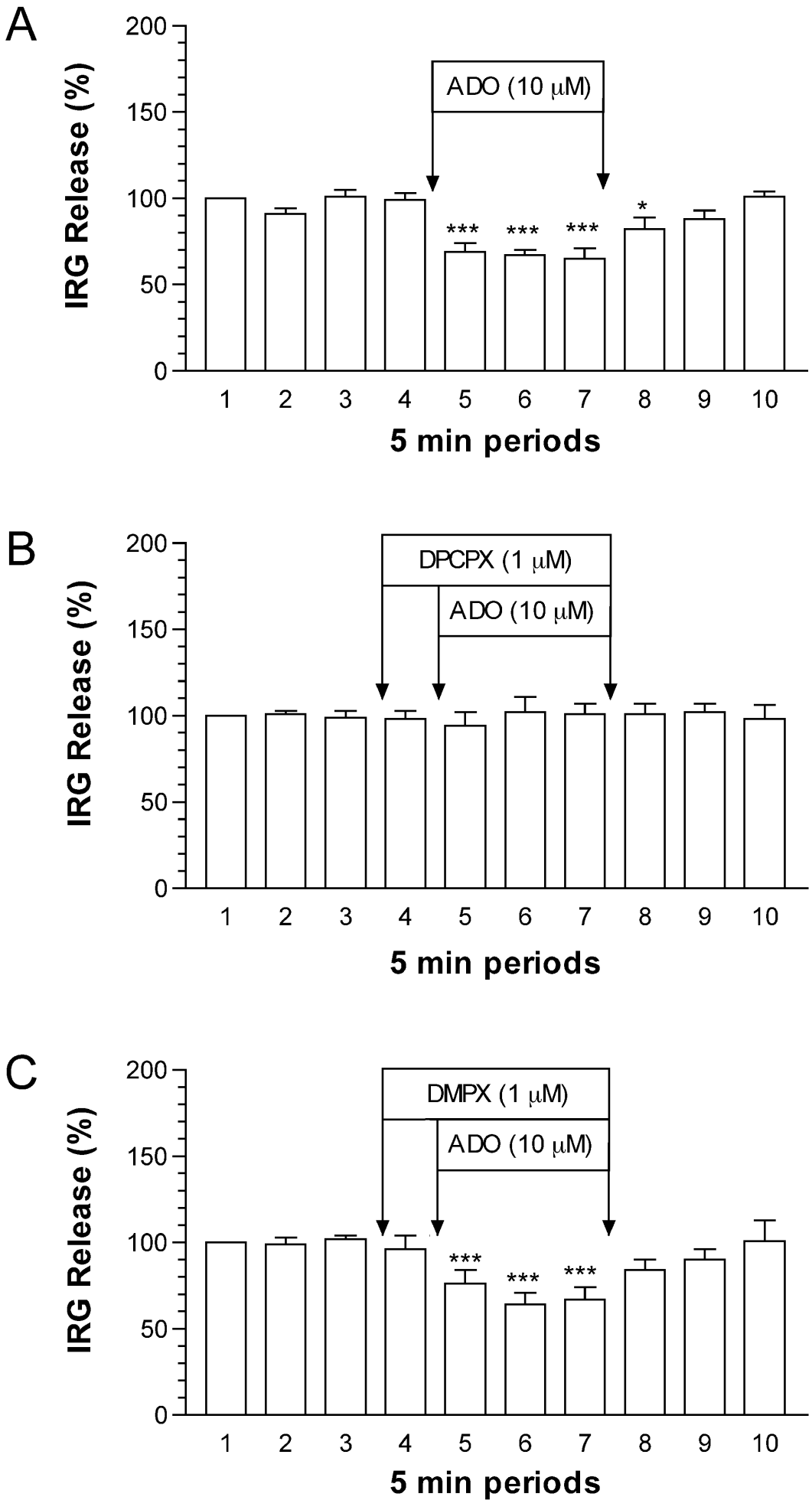

Fig. 4

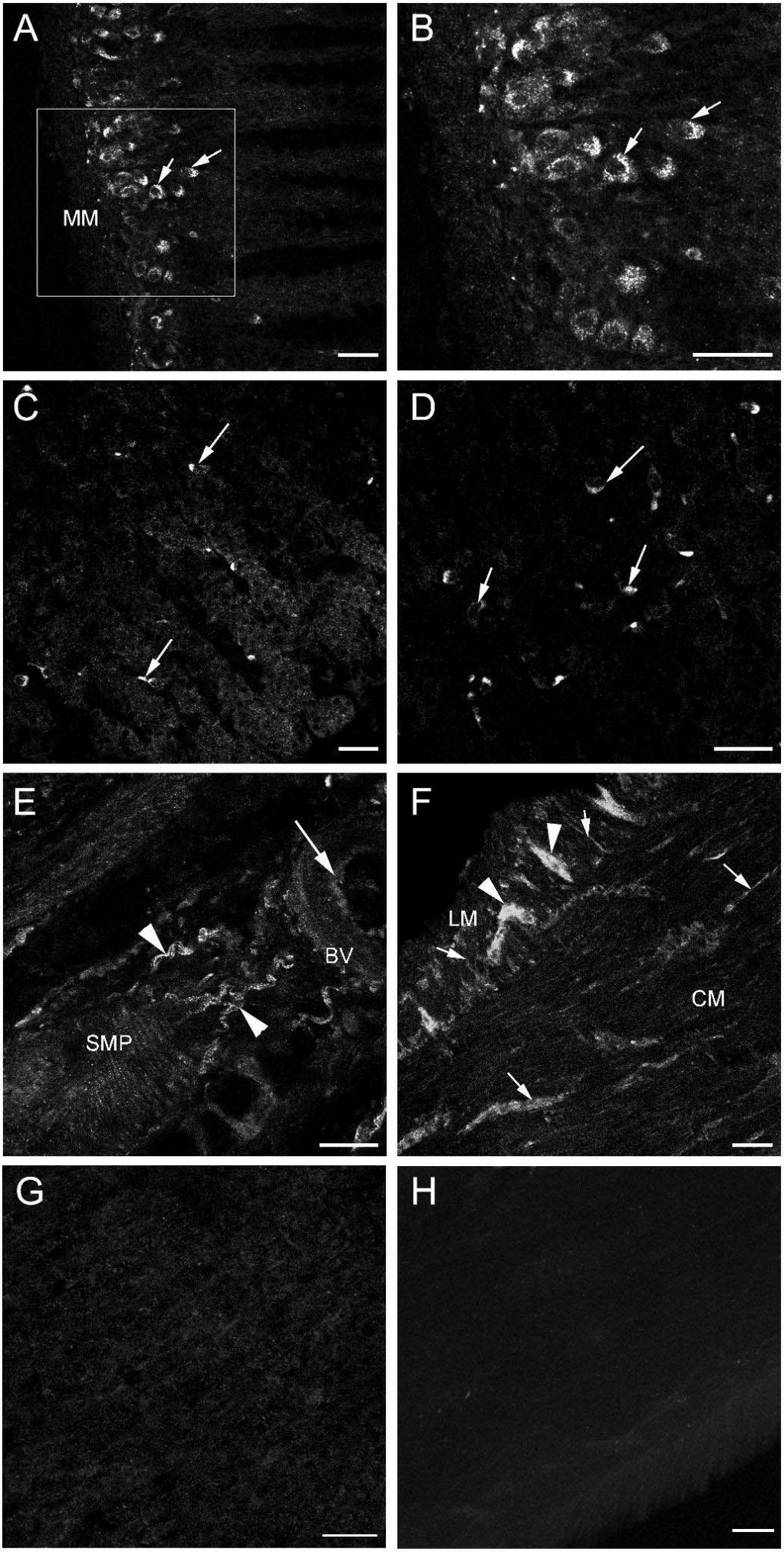

Fig. 5

Fig. 6

JPET Fast Forward. Published on March 24, 2004 as DOI: 10.1124/jpet.104.066654
This article has not been copyedited and formatted. The final version may differ from this version.

JPET Fast Forward. Published on March 24, 2004 as DOI: 10.1124/jpet.104.066654

Fig. 7

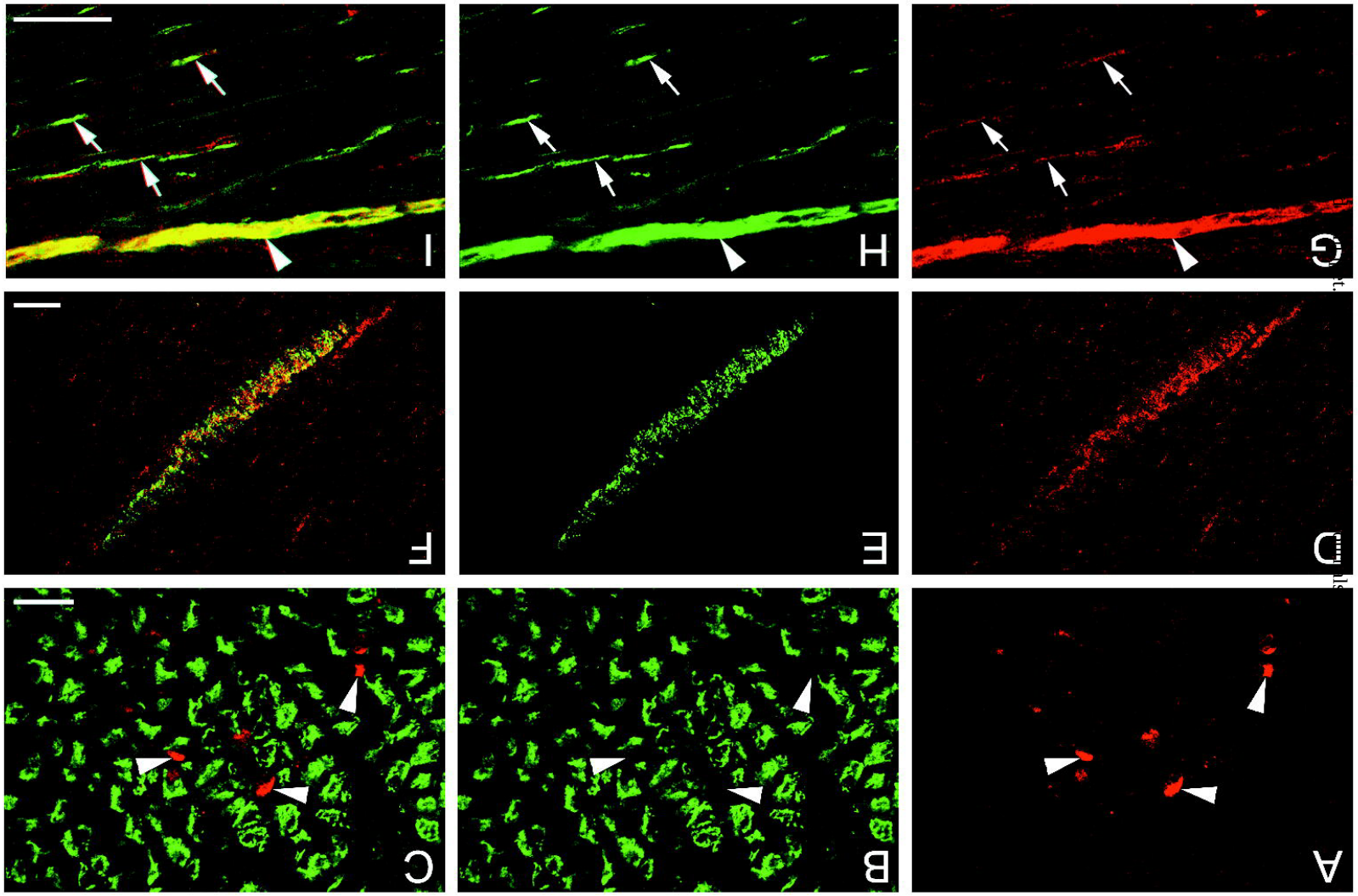

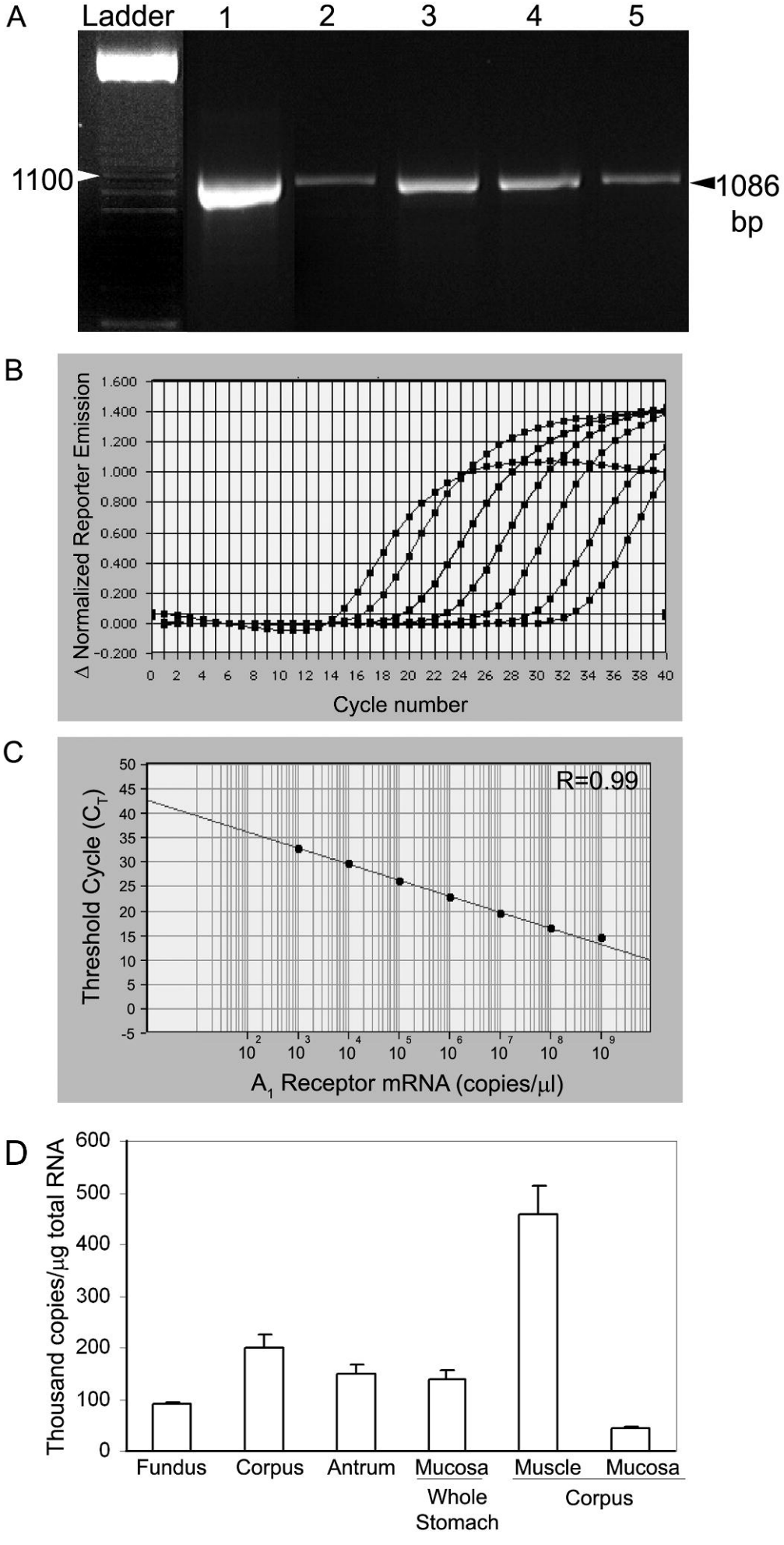

Fig. 8